LAWRENCE
LIVERMORE
NATIONAL
LABORATORY

LLNL-CONF-555952

Neutron spectrometry - An essential tool for diagnosing implosions at the National Ignition Facility

A. J. Mackinnon, M. Gatu Johnson, J. A. Frenje, D. T. Casey, C. K. Li, F. H. Seguin, R. Petrasso, R. Ashabranner, C. Cerjan, T. J. Clancy, R. Bionta, D. Bleuel, E. J. Bond, J. A. Caggiano, A. Capenter, M. J. Eckart, M. J. Edwards, S. Friedrich, S. H. Glenzer, S. W. Haan, E. P. Hartouni, R. Hatarik, S. P. Hachett, M. McKernan, O. Jones, S. Lepape, R. A. Lerche, O. L. Landen, M. Moran, E. Moses, D. Munro, J. McNaney, J. R. Rygg, S. Sepke, B. Spears, P. Springer, C. Yeamans, M. Farrell, J. D. Kilkenny, A. Nikroo, R. Paguio, J. Knauer, V. Glebov, T. Sangster, R. Betti, C. Stoeckl, J. Magoon, M. J. Shoup, G. P. Grim, G. L. Moran, T. J. Murphy, R. J. Leeper, C. Ruiz

May 7, 2012

19th Topical Conference High-Temperature Plasma Diagnostics
Monterey, CA, United States
May 6, 2012 through May 10, 2012

Disclaimer

Neutron spectrometry - An essential tool for diagnosing implosions at the National Ignition Facility (invited)[a)]

M. Gatu Johnson,[1,b] J. Frenje,[1] D.T. Casey,[1] C.K. Li,[1] F.H. Séguin,[1] R. Petrasso,[1] R. Ashabranner,[2] R. Bionta,[2] D. Bleuel,[2] E.J. Bond,[2] J.A. Caggiano,[2] A. Carpenter,[2] C.J. Cerjan,[2] T.J. Clancy,[2] M.J. Eckart,[2] M.J. Edwards,[2] S. Friedrich,[2] S.H. Glenzer,[2] S.W. Haan,[2] E.P. Hartouni,[2] R. Hatarik,[2] S.P. Hatchett,[2] O.S. Jones,[2] S. Le Pape,[2] R.A. Lerche,[2] O.L. Landen,[2] A.J. MacKinnon,[2] M. McKernan,[2] M.J. Moran,[2] E. Moses,[2] D.H. Munro,[2] J. McNaney,[2] J.R. Rygg,[2] S.M. Sepke,[2] B. Spears,[2] P.T. Springer,[2] C. Yeamans,[2] "...", M. Farrell,[3] J.D. Kilkenny,[3] A. Nikroo,[3] R. Paguio,[3] "...", J.P. Knauer,[4] V. Yu Glebov,[4] T.C. Sangster,[4] R. Betti,[4] C. Stoeckl,[4] J. Magoon,[4] M.J. Shoup,[4] "...", G.P. Grim,[5] G.L. Morgan,[5] T.J. Murphy,[5] "...", R.J. Leeper,[6] C.Ruiz[6] and "..."

[1]*Massachusetts Institute of Technology Plasma Science and Fusion Center, Cambridge MA 02139, USA*
[2]*Lawrence Livermore National Laboratory, Livermore, CA 94550, USA*
[3]*General Atomics, San Diego, CA, USA*
[4]*Laboratory for Laser Energetics, University of Rochester, Rochester, NY 14623, USA*
[5]*Los Alamos National Laboratory, Los Alamos, NM, 87545*
[6]*Sandia National Laboratory, New Mexico 87123, USA*

(Presented XXXXX; received XXXXX; accepted XXXXX; published online XXXXX)

DT neutron yield (Y_n), ion temperature (T_i) and down-scatter ratio (*dsr*) determined from measured neutron spectra are essential metrics for diagnosing the performance of Inertial Confinement Fusion (ICF) implosions at the National Ignition Facility (NIF). A suite of neutron-Time-Of-Flight (nTOF) spectrometers and a Magnetic Recoil Spectrometer (MRS) have been implemented in different locations around the NIF target chamber, providing good implosion coverage and the redundancy required for reliable measurements of Y_n, T_i and *dsr*. From the measured *dsr* value, an areal density (ρR) is determined from the relationship ρR_{tot} (g/cm^2) = (20.4±0.6)×$dsr_{10\text{-}12\ MeV}$. The proportionality constant is determined considering implosion geometry, neutron attenuation and energy range used for the *dsr* measurement. To ensure high accuracy in the measurements, a series of commissioning experiments using exploding pushers have been used for *in situ* calibration. The spectrometers are now performing to the required accuracy, as indicated by the good agreement between the different measurements over several commissioning shots. In addition, recent data obtained with the MRS and nTOFs indicate that the implosion performance of cryogenically layered DT implosions, characterized by the experimental Ignition Threshold Factor (ITFx) which is a function of *dsr* (or fuel ρR) and Y_n, has improved almost two orders of magnitude since the first shot in September, 2010.

I. INTRODUCTION

Hot-spot ignition planned at the National Ignition Facility[1] (NIF) requires the formation of a round, high temperature hot-spot surrounded by high fuel areal density (ρR). Experimental information about yield (Y_n), ion temperature (T_i), ρR and ρR asymmetries are critical for diagnosing implosion performance and for understanding how the fuel assembles. To obtain this information, a suite of neutron spectrometers have been implemented and extensively used on the NIF for measurements of the neutron spectrum in the energy range from 1.5 to about 20 MeV. This range covers all essential details of the neutron spectrum, allowing for simultaneous determination of ρR, T_i, Y_n, and possible non-thermal features in the implosion. From the primary neutron spectrum, T_i and Y_n are determined, and from the ratio between down-scattered and primary neutrons, the down-scattered ratio (*dsr*) is determined, which is to the first order proportional to the fuel ρR. The neutron spectrometers are part of a neutron diagnostic suite,[2] which also includes neutron activation detectors (NADS)[3] for yield measurements, and a Neutron Imaging System (NIS)[4] for measurements of the spatial distribution of the primary-neutron source and down-scattered neutron source.

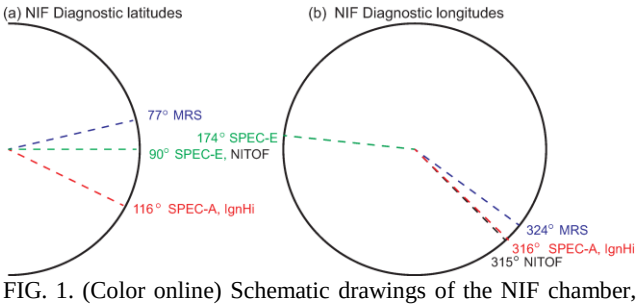

FIG. 1. (Color online) Schematic drawings of the NIF chamber, indicating the different lines of sight (LOS) for the nTOF and MRS neutron spectrometers. (a) Side projection. (b) Top view. The different locations of the spectrometers provide improved coverage of the implosion.

[a)]Invited paper published as part of the Proceedings of the 19th Topical Conference on High-Temperature Plasma Diagnostics, Monterey, California, May, 2012.
[b)]Author to whom correspondence should be addressed: gatu@psfc.mit.edu.

The neutron spectrometers, which include several neutron Time-of-Flight (nTOF) detectors[5,6,7] and a Magnetic Recoil neutron Spectrometer (MRS),[8,9,10,11] are fielded at different locations around the implosion for directional measurements of the neutron spectrum (fig. 1).

This ensures good coverage of the implosion, allowing for determination of ρR asymmetries[12] and possible non-thermal effects. The diametrically different detection principles of the MRS and nTOF techniques add to the reliability of, and redundancy in, the neutron spectrum measurements.

To achieve the required accuracy for the measurement of the absolute neutron spectrum, a set of commissioning experiments was conducted on the NIF for an *in situ* calibration and characterization of the different spectrometers. With the spectrometers fully commissioned, they are now used routinely in support of the National Ignition Campaign (NIC),[13] providing results that have been essential to the progress of the NIC toward demonstrating ignition.

The individual measurements of Y_n, T_i and *dsr* are weighted together, taking into account their errors, to get an average value that better represents the overall implosion performance. This average value is robust due to the large implosion coverage and the varying detection principles of the different instruments.

This paper is structured as follows. Section II describes the ICF neutron spectrum. Aspects of the *dsr* measurement and how it relates to the total and DT-fuel ρR are also discussed in this section. Section III discusses the neutron spectrometer commissioning experiments, and Section IV presents spectrometry data from cryogenically layered DT implosions.

II. THE ICF NEUTRON SPECTRUM

The ICF neutron spectrum has been frequently described elsewhere,[5,9,12] and is therefore only discussed briefly in this paper. The D(T,n)α reaction produces primary neutrons with a zero-temperature kinetic energy of 14.03 MeV. As the DT reactions occur in a hot plasma, the primary neutron spectrum is Doppler broadened and energy upshifted due to a finite effective T_i. For a single-temperature plasma, T_i is determined from the Doppler width ($\Delta E_n^{\mathrm{FWHM}}$) of the primary neutron spectrum, which is well represented by a Gaussian distribution [T_i is to the first order equal to $(\Delta E_n^{\mathrm{FWHM}}/177)^2$ keV][14]. Temperature profiles or non-thermal reactions result in deviations from the single-Gaussian distribution. Non-thermal effects could, for instance, be caused by bulk flows in the fuel at velocities as high as the sound speed. Scattering in the cold, dense fuel and ablator that surrounds the hot spot gives rise to a low energy (down-scattered) component in the neutron spectrum. The physical quantity measured by the neutron spectrometers is the down-scattered ratio, which is defined as $dsr(E)_{\mathrm{exp}}=Y(E)/Y_{n,13\text{-}15\ \mathrm{MeV}}$, while hydrodynamic codes simulate compression performance given in ρR. Fig. 2a shows MCNPX[15] simulated neutron spectra for implosions with ρR varying in the range 0.1 – 2.0 g/cm^2 (T_i = 3 keV). As shown, both shape and magnitude of the down-scattered neutron spectrum changes significantly with increasing ρR. As discussed in refs [9,12,16], the magnitude of the down-scattered neutron spectrum (10-12 MeV) relative to the neutron yield, or dsr_{exp}, is to the first order proportional to ρR. The conversion factor (C) between the fuel ρR and down-scatter ratio, $dsr(E)=Y(E)/Y_{\mathrm{tot}}$ (where Y_{tot} is the total number of DT neutrons produced in the implosion), has been derived analytically[9] for a neutron point source (ps) and a 50:50 DT plasma to be

$$\rho R_{DT}^{ps} \approx \frac{5m_p}{\sigma_{nd}(E)+\sigma_{nt}(E)}\, dsr(E) = C \times dsr(E), \qquad (1)$$

where m_p is the proton mass and $\sigma(E)$ is the energy dependent cross sections for elastic n,D and n,T scattering and $(n,2n)$ breakup reactions in D and T. These nuclear processes contribute to the measured low energy neutron spectrum and need to be included when integrating the cross sections over the appropriate energy interval. As the analytical expression in eq. 1 only considers single scattering for a low ρR case, it needs to be modified to take into account (i) multiple scattering, (ii) attenuation of primary and down-scattered neutrons, (iii) the effect of ablator ρR, and (iv) the effect of implosion geometry (size and shape of the primary and scattering sources). As ρR increases, multiple scattering and attenuation increase in importance, especially at neutron energies below ~8 MeV, resulting in a change in spectral shape. This is clearly shown in fig. 2b, which illustrates the primary neutron component, single-scattering component, and multiple-scattering component for ρR=0.2 and ρR=2.0 g/cm^2 implosions. In addition, because of significant multiple scattering and attenuation in high-ρR implosions at the NIF, the measured yield $Y_{n,13\text{-}15\ \mathrm{MeV}}$ does not well represent the total yield used in eq. 1.

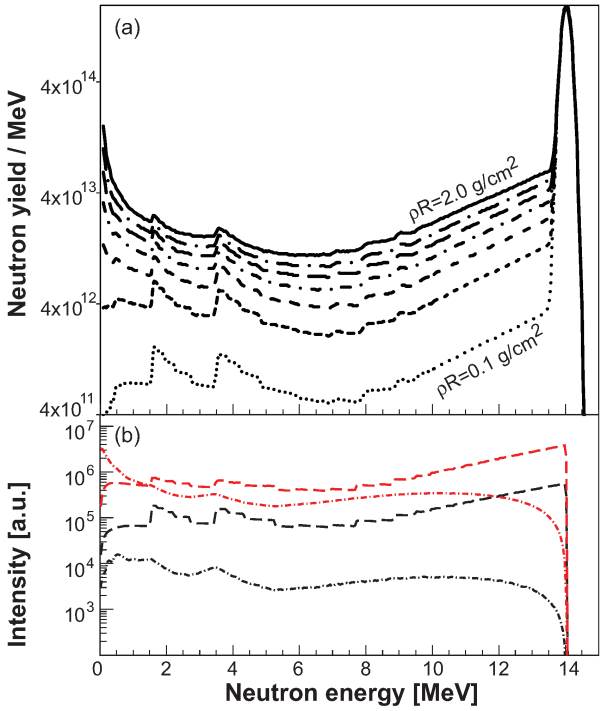

FIG. 2. (Color) (a) Simulated neutron spectra, normalized to a neutron yield of 7×10^{14} in the 13-15 MeV region. These simulations used a T_i =3 keV DT neutron point source in the center of a spherical high-density DT shell with inner and outer radii of 30 and 50 μm, and with varying ρRs (0.1, 0.4, 0.7, 1.0, 1.3, 1.6 and 2.0 g/cm^2). The shape and magnitude of the down-scattered neutron spectrum changes as a function of ρR. (b) Simulated single-scattered (dashed line, also including D(n,2n) neutrons) and multi-scattered (broken line) neutron spectra from a mono-energetic point source in a sphere with ρR=0.2 (black) and ρR=2.0 (red) g/cm^2. As can be seen, the multi-scatter contribution increases significantly with ρR, especially at energies below ~8 MeV.

At bang time, some of the ablator mass needs to be preserved to control hydrodynamic instabilities in the implosion.[16] This remaining mass will contribute to the down-scattered neutron signal, but on a level much lower than the

down-scattered neutron signal from the DT fuel. This is due to the smaller cross sections for the ablator material per mg/cm^2. If we assume a CH ablator (which is currently used on the NIF) and a relative ρR contribution from CH of $X=\rho R_{CH}/\rho R_{DT}$, then the fractional CH contribution to the observed $dsr_{10\text{-}12\ MeV}$ can be written as

$$dsr_{CH} \approx \frac{5\sigma_{CH}(E)}{13\sigma_{DT}(E)} X \times dsr_{DT} \overset{10-12MeV}{\approx} 0.12X \times dsr_{DT,10-12MeV}. \quad (2)$$

X has been estimated from LASNEX simulations[17] to be ~0.1, which means that ~ 1%, of the observed $dsr_{10\text{-}12\ MeV}$ will be due to the CH ablator. This, however, means that the CH ρR is not well probed by down-scattered neutrons and needs to be measured in other ways, such as with knock-on protons[18], gamma-ray spectroscopy[19] or x-ray methods[20].

In realistic implosion geometries, the average neutron path lengths through the dense fuel are generally longer than in the point-source case, leading to higher measured *dsr* values for a given ρR, and a reduced conversion factor. LASNEX simulations of numerous NIF implosions were used to derive the following conversion factors for the total and DT-fuel ρR:

$$\rho R_{tot}\ (g/cm^2) = (20.4\pm0.6)\times dsr_{10\text{-}12\ MeV} \quad (3)$$
$$\rho R_{fuel}\ (g/cm^2) = (18.8\pm0.5)\times dsr_{10\text{-}12\ MeV.} \quad (4)$$

In these simulations, X was determined to be 0.08±0.04.

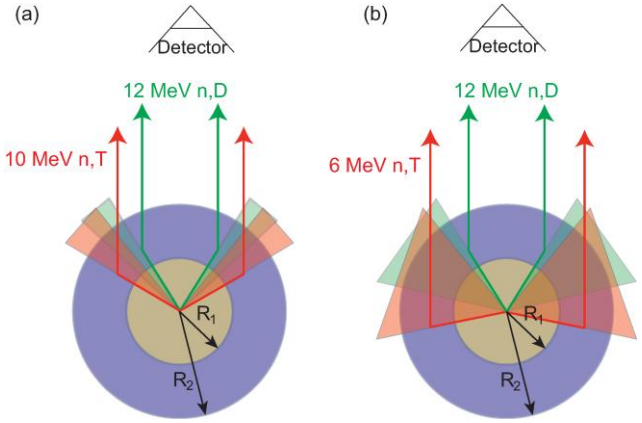

FIG. 3. (Color) Implosion region sampled when using (a) the $E_{n'}$=10-12 MeV and (b) the $E_{n'}$=6-12 MeV range for the *dsr* measurement. The implosion fraction sampled is 17% and 53% for 10-12 MeV and 6-12 MeV, respectively. For the determination of an average ρR that better represents the implosion performance, the 6-12 MeV energy range is preferable. Currently, 10-12 MeV is used for *dsr* measurements, but this measurement will be complemented by other *dsr* measurements in the near future. These schematic drawings only consider single *n,D* elastic scattering (green), *n,T* elastic scattering (red), a point source, and a dense DT shell.

The part of the implosion sampled by a spectrometer depends primarily on the *dsr* energy range used, composition of the fuel and ablator material, energy dependence of the differential cross section for the different nuclear processes, and implosion geometry. When only considering *n,D* and *n,T* elastic scattering (and not the (n,2n) processes), the sampled angular interval for a given scattered neutron energy range can be determined from the (non-relativistic) relationship

$$E_{n'} = \frac{1}{(A+1)^2} E_n \left(\cos\theta + \left(A^2 - \sin^2\theta\right)^{\frac{1}{2}} \right)^2. \quad (5)$$

Here, $E_{n'}$ is the energy of the down-scattered neutron, θ is the neutron scattering angle in the lab system, and A the mass number of the scattered nucleus. Using eq. (5), the sampled angular ranges for $E_{n'}$=10-12 MeV and $E_{n'}$=6-12 MeV can be illustrated for a neutron point source as in fig. 3. For a more realistic implosion geometry, the fraction of the implosion sampled is increased relative to the point source case (see fig. 4).

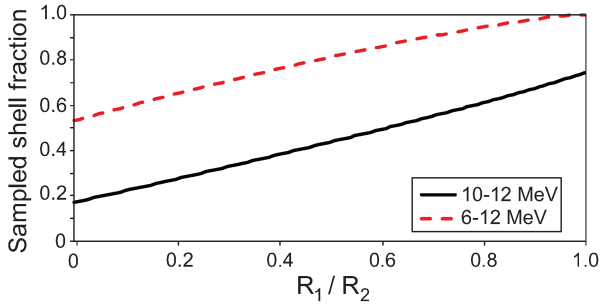

FIG. 4. (Color online) Implosion coverage when using 10-12 MeV and 6-12 MeV for the dsr measurement as functions of the ratio between primary-source radius (R_1) and cold fuel radius (R_2). Only single scattering is considered, and it is assumed that both radii are measured from the implosion center. In the zero limit, this treatment is reduced to the scenario shown in fig. 3.

Currently, E_n=10-12 MeV is used for *dsr* measurements, but broader or different energy ranges have been used and will be routinely used in the near future. Ultimately, the plan is to use the whole neutron spectrum down to thermal energies[21] to extract as much information as possible about the implosion.

III. COMMISSIONING EXPERIMENTS

The different neutron spectrometers were installed and commissioned on the NIF in stages. The nTOFs were installed in 2009 and 2010, the MRS in late 2010 and NITOF in 2011. These spectrometers were commissioned over a time period of about 6-12 months, during which the systems were calibrated *in situ* in a coordinated fashion. In this section, the commissioning experiments are discussed in some detail. Common to all is that a series of exploding pusher implosions[22] were used to calibrate or verify the performance of the spectrometers before they were used to diagnose layered DT implosions.

A. MRS

As the principle of the Magnetic Recoil neutron Spectrometer (MRS) has been described in detail elsewhere[8,9,10,11], it is only discussed briefly in this paper. The system consists of four main components: a 13 cm^2 deuterated polyethylene foil (CD_2) positioned 26 cm from Target Chamber Center (TCC), a focusing magnet, made of Nd-Fe-B, positioned just outside the NIF chamber, an array of nine CR-39 detectors positioned at the magnet focal plane, and 6000 lbs of polyethylene shielding fully enclosing the spectrometer. The principle of the MRS is as follows. A small fraction of the emitted neutrons hit the CD_2 foil and produce elastically scattered deuterons. Forward-scattered deuterons are selected by an adjustable-sized magnet aperture positioned in front of the magnet. Selected deuterons are momentum analyzed and focused onto the CR-39 detector array. The position of the detected deuteron depends on its energy. The CR-39 detectors are processed in dedicated etch and scan labs, and then analyzed to

reconstruct the recoil deuteron spectrum, from which the neutron spectrum is inferred (currently using a forward-fitting technique).

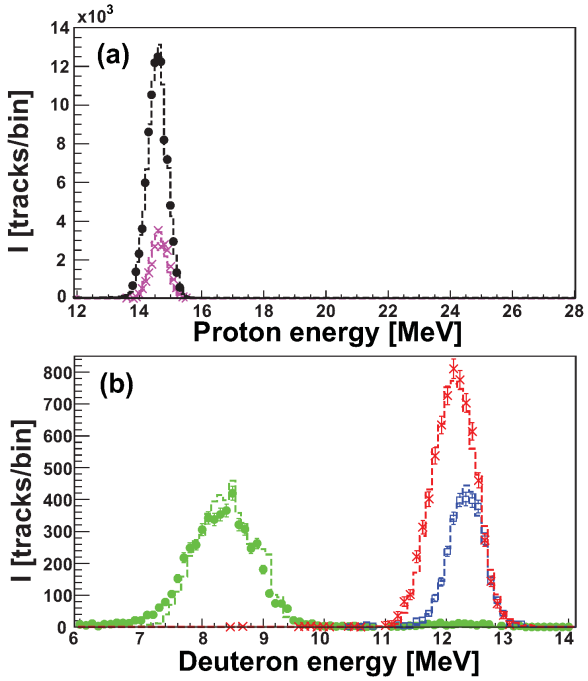

FIG. 5. (Color online) (a) Primary measured D^3He proton spectra for D^3He exploding pusher shots N100823 (black circles) and N110722 (magenta crosses). (b) Measured recoil deuteron spectra for DT exploding pusher shots N101030 (red crosses), N110217 (blue squares) and N101212 (green circles). The spectrum for N101212 was obtained by positioning a 75 μm Ta filter behind the CD_2 foil, ranging the deuterons down to ~8.5 MeV. As the filter did not cover the foil entirely, both ranged-down and non-ranged down deuterons were detected simultaneously. The spectra in (a) and (b) are overlayed (not fit) with Geant4 simulations of the setup for each shot (dashed lines). The simulations reproduce the measured energy distributions over the full range to an accuracy of ±50 keV neutron energy equivalent. Note that energy ranges corresponding to the same physical range are shown in (a) and (b); deuterons fall at a location approximately corresponding to that of protons of double the energy due to the 2:1 mass ratio.

The efficiency of the MRS can be accurately calculated *ab initio*, allowing the MRS to provide a solid, independent Y_n measurement.[23] Spectral broadening due to geometry, CD_2 foil thickness and magnet properties determines the spectrometer resolution. In standard fashion, the efficiency can be increased at the expense of resolution by using a thicker CD_2 foil. To date, the MRS has been operated with six different foils, manufactured by General Atomics, ranging from ~50 to 250 μm in thickness. In addition, the MRS can be operated without a conversion foil on exploding pushers for measurements of charged particles (e.g., 14.7 MeV protons from D^3He reactions) emitted directly from the implosion.

An accurate reconstruction of the neutron spectrum from the measured deuteron spectrum requires detailed knowledge about the instrument response function (IRF), which is calculated *ab initio* based on the MRS geometry and measured magnetic field map. The calculated IRF requires verification through *in situ* measurements to establish the as-built properties of the system. The MRS was first operated, without the CD_2 conversion foil, on a D^3He Exploding Pusher (Shot N100823, fig 5a). Measured data from this shot conclusively verified that the proton distribution in the non-dispersion direction agreed with *ab initio* simulations, indicating that the MRS was well aligned. In addition, solid calibration data were obtained on a series of D^3He (fig. 5a) and DT (fig. 5b) exploding pushers. On DT shot N101030, the MRS was fielded in medium resolution mode (~140 μm foil thickness, ΔE_{MRS}≈1100 MeV Full Width Half Maximum (FWHM)), on DT shot N101212 it was fielded in medium resolution mode with a 75 μm Ta ranging filter behind the foil to get a calibration point at ~8.5 MeV deuteron energy, on DT shot N110217 it was fielded in high resolution mode (~50 μm foil thickness, ΔE_{MRS}≈510 MeV FWHM), and on D^3He shot N110722 it was fielded with a 196 μm Stainless Steel paddle with a hole to give D^3He protons at nominal energies of 14.7 MeV and 11.3 MeV (the lower energy point is not shown in fig. 5). It was found that the complete set of data, including the D^3He point ranged down through 196 μm SS, could be accurately described over the full energy range covered in these experiments to within ±50 keV neutron energy equivalent if the magnetic field strength as given by the manufacturer, Dexter Magnetic Technologies Inc., was increased by 4.95%. The average DT peak location for layered cryogenic implosions falls 0.7 keV from nominal.

The MRS was carefully designed to minimize scattering materials between TCC and the CD_2 foil to avoid any background interference in the low energy down-scattered neutron region, which could compromise the *dsr* measurement. It was also designed to reduce the ambient neutron background to the required level. Data from two DT exploding pushers (N101030 and N110217), in which the ρR is negligibly small, were used as a "null" test to ensure the quality of the MRS *dsr* measurement. The inferred $dsr_{10\text{-}12\ MeV}$ for N101030 and N110217 is 0.1%±65% and -0.2%±260%, respectively, indicating that the background interference of the *dsr* measurement is insignificant.

B. nTOF

The suite of nTOF spectrometers includes a total of 12 instruments for diagnosing the neutron emission from DD and DT implosions with neutron yields ranging from 10^8-10^{19}.[5] In this paper, we focus on the nTOFs used for DT Y_n, T_i and *dsr* measurements. These currently include two liquid scintillators (Spec-A and Spec-E) at about 20 m from TCC, a set of CVD diamonds at 20 m (IgHi) and a plastic scintillator at 27.3 m (NITOF). All nTOFs consist either of a fast CVD diamond or a scintillator detector coupled to a photodiode (PD) or photomultipler tube (PMT), biased to high voltage. Each nTOF is operated in current mode with the signal collected on one or more oscilloscopes. With a fixed and well-known distance to TCC, known IRF (discussed later), and taking the mean primary neutron energy as given, the neutron spectrum can be inferred from the time-of-flight spectrum.

As an accurate absolute yield calibration could not be applied to the nTOF detectors, they were cross-calibrated to the weighted average yield measured with the MRS and Zr and Cu Neutron Activation (NADS)[3] on DT Exploding pushers. The yield calibration is continuously checked as new data is collected.

1. nTOF20m-SPEC detectors

The nominally identical Spec detectors, located at 20 m from TCC in the neutron alcove (A) and on the equator (E), are the workhorse nTOF detectors designed to measure the neutron spectrum in the range 1.5-15 MeV and to provide accurate *dsr* and T_i measurements. They are oxygen-quenched xylene-based liquid scintillators[5] with a relatively narrow response (5 ns),

coupled to two photomultiplier tubes, PMT140 and PMT240, with different gains. The less-sensitive PMT140 (gain 10^3) is used to record the high-intensity neutron spectra from DT implosions, while the more-sensitive PMT240 (gain 10^5) is gated to only measure the spectrum below ~4 MeV, avoiding saturation from the 14-MeV neutrons.[6] The PMT140 is primarily used for the primary neutron and 10-12 MeV *dsr* measurement. Its sensitivity is limited in the E_n<4 MeV region due to dynamic range. The PMT240 is used to record the DD spectrum in a DT background and *n,D* and *n,T* elastic back-scatter edges (the backscatter measurement is discussed in detail in [24]) .

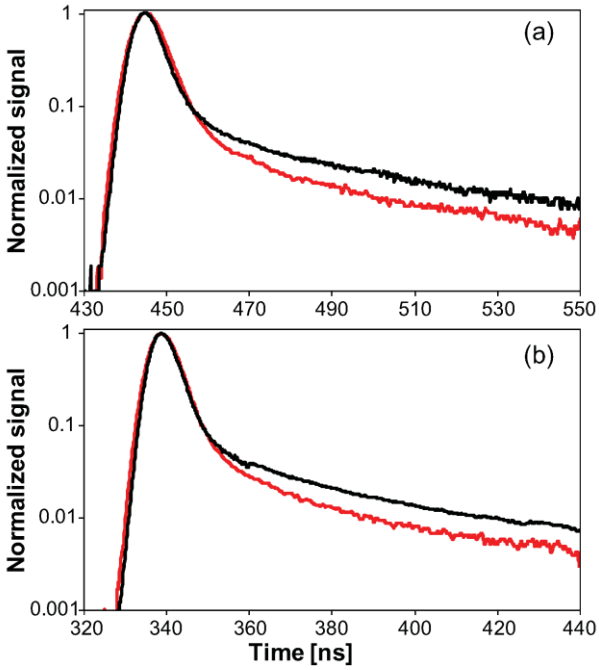

FIG. 6. (a) Example nTOF Spec-A traces for a low-ρR exploding pusher (N111121, red) and a high-ρR DT layered shot (N111112, black). (b) Spec-E traces for the same shots. The difference in tail intensity is due to down-scattered neutrons (480-523 ns for Spec-A and 370-410 ns for Spec-E corresponds to E_n~10-12 MeV).

An X-ray burst of ~90 ps emitted from a planar-foil experiment on the NIF was used to determine the impulse response of the Spec-A and Spec-E detectors, including cables, scintillators and PMTs. To also account for scattering of 14 MeV neutrons in the LOS and scintillator response to neutrons, these impulse response measurements were convolved with the result from neutron transport calculations and scintillator light yield calculations for 14 MeV neutrons to determine the IRFs. In addition to the primary interaction with the scintillator, these calculations include secondary generation of x-rays due to the interaction of neutrons with structures defining the LOS and structures surrounding the nTOF detector. The accurately determined IRFs for Spec-A and Spec-E allow for an independent T_i measurement (accuracy ~12%). Signal intensity for a given neutron yield was, on the other hand, determined through cross calibration to NADS and MRS yield measurements on DT exploding pushers, as described above. The DT-primary signal decay (including contributions from scintillator afterglow, PMT response and neutron scattering) was measured using "null ρR" DT exploding pushers to determine the background level for the *dsr* measurements on cryogenically layered DT shots. Figure 6 shows examples of nTOF Spec-A and Spec-E traces from a low-ρR exploding pusher (N111121) and a high-ρR layered DT shot (N111112). The difference in signal level in the time window 479-523 ns (Spec-A) and 370-410 ns (Spec-E), corresponding to 10-12 MeV neutrons, represents down-scattered neutron signal from the DT layered shot. The uncertainty in the *dsr* measurements is ~10%, taking into account uncertainty in the exploding pusher baseline measurement.

2. nTOF20m-Ignition High

The "ignition high" (IgHi) detector[5] is positioned 20 m from TCC in the neutron alcove. It consists of a set of four CVD diamonds of varying size and sensitivity. At current yields (<10^{15}), only the most sensitive diamond with 24 mm diameter and 1 mm thickness is providing good signal. IgHi has a very fast and narrow response (3.3 ns for the 24 mm detector, 1.2 ns for the 10 mm detectors), allowing for accurate T_i measurements. The IgHi IRF is constructed from x-ray response measurements using a diamond located at ~4 m from TCC (nTOF BT[5]), convolved with the known IgHi cable response. As for the Spec-A and Spec-E detectors, the low-energy baseline signal is determined from DT exploding pusher measurements, allowing for a *dsr* determination from IgHi data (uncertainty ~10%). As for the other nTOFs, a yield calibration of the IgHi detectors is done using MRS and NADS data (accuracy of a few percent).

3. NITOF

The Neutron Imager Time-Of-Flight (NITOF) detector is a current mode NE-111 plastic-scintillator based detector fielded on the equator in the same LOS as the Neutron Imaging System at 27.3 m from TCC. This system is designed for T_i and *dsr* measurements. The IRF (width 2.17 ns FWHM) is independently constructed from primary-peak x-ray response measurements on OMEGA (first decay constant), combined with scintillator decay property measurements using neutrons from an AmBe source at LANL (two longer decay constants).

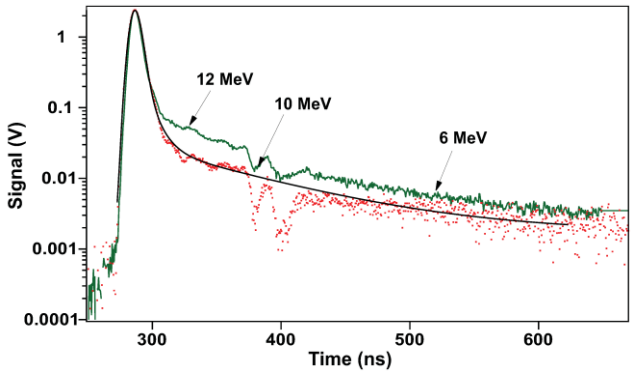

FIG. 7. (Color) Example of NITOF data from DT Exploding Pusher shot N111121 (red) and DT layered shot N111215 (green, time shifted -20 ns to match N111121). The black curve represents the best-fit to the exploding pusher data using the IRF. The N111121 13-15 MeV intensity is renormalized to N111215. The intensity difference in the 6-12 MeV equivalent region (indicated in the figure) is due to down-scattered neutrons. Note that the NITOF baseline level on the layered shot is not determined from exploding pusher data, but using identical out-of-beam detectors fielded on the same shot.

DT exploding pusher data are accurately described by adjusting the width and amplitude of the IRF, as shown for N111121 in figure 7, where data from layered shot N111215 is also shown for comparison. Unlike the other nTOF detectors, the NITOF low energy baseline level is not determined from DT exploding pusher measurements. The background subtraction for

the *dsr* measurement is done using data taken from equivalent out-of-beam detectors fielded on the same shot. The main background of scattered neutrons comes from the Neutron Imaging System itself. With its independent IRF calibration and unique scheme for *dsr* determination, NITOF adds important redundancy for the *dsr* and T_i measurements (absolute accuracy 0.5% and 0.5 keV, respectively). NITOF is currently not calibrated to provide Y_n.

IV. DIAGNOSING CRYOGENICALLY LAYERED DT IMPLOSIONS

The suite of neutron spectrometers has been used to diagnose some thirty cryogenically layered implosions from the first dudded pre-tuning THD implosions in 2010 and early 2011[25,26] through to the more recent cryogenically layered 50:50 DT implosions in Uranium Hohlraums. These measurements have been essential for diagnosing the implosion performance, characterized by the experimental Ignition Threshold Factor (ITFx),[16,27,28] and for guiding NIC towards the first demonstration of ignition in a laboratory. The ITFx has improved from 1.5×10^{-3} on N100929 to ~0.1 on N120321.

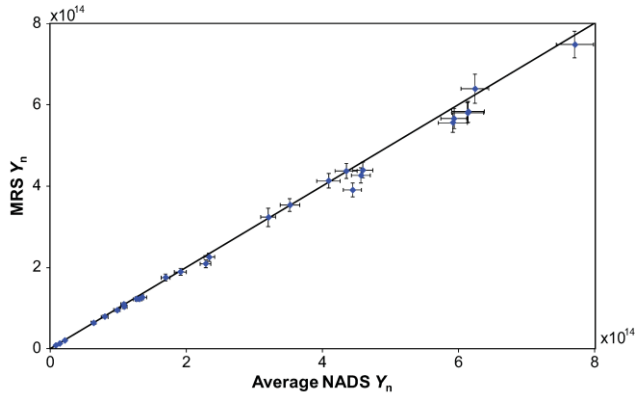

FIG. 8. (Color online) Primary neutron yields measured with MRS compared to average NADS yields (blue diamonds) for DT layered shots. Also shown is the 45° line (black).

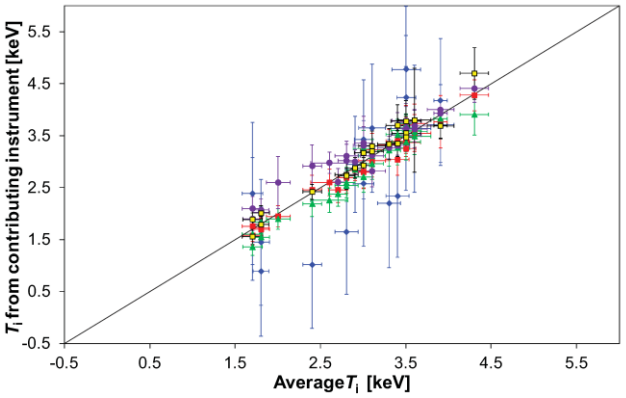

FIG. 9. (Color) Ion temperatures measured with MRS (blue diamonds), Spec-A (red squares), Spec-E (green triangles), IgHi (purple circles) and NITOF (black/yellow squares) as a function of the average T_i for all layered DT shots.

Figure 8 shows the primary neutron yield measured with the MRS compared to the weighted average NADS yield value (including Cu and Zr NADS data) for all layered shots. (Recall that the nTOFs are not absolutely yield calibrated.) The plot shows consistent agreement over a large yield range.

The Spec-A, Spec-E, IgHi, NITOF and MRS IRFs are independently determined for T_i measurements. The T_i results from these detectors are contrasted to the average T_i in Fig. 9. The agreement between the Spec-A, Spec-E and NITOF measurements is remarkable, given the different methods for determining the IRF. The error bars for MRS T_i data are large because the primary neutron yields have been $<10^{15}$, which requires the MRS to be operated in medium-resolution mode.

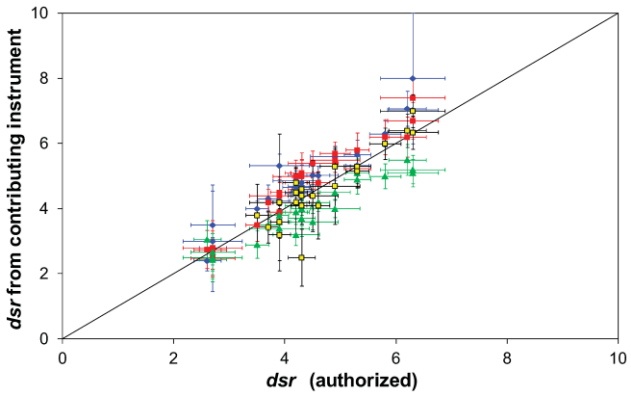

FIG. 10. (Color) *dsr* (10-12 MeV) values measured with the MRS (blue diamonds), Spec-A (red squares), Spec-E (green triangles) and NITOF (yellow/black squares) as a function of average *dsr* (solid black line).

Figure 10 shows the *dsr* (10-12 MeV) results measured with the MRS, Spec-A, Spec-E and NITOF as a function of the average *dsr* value. As shown by the data, the SPEC-E *dsr* data is systematically lower than *dsr* from the other spectrometers, which is now believed to be a real effect (possible ρR asymmetry), but further investigations are required before any final conclusions can be drawn. The issue is currently being addressed by analyzing all the *dsr* data over a wider energy range, which corresponds to larger coverage of the implosion (figs. 3 and 4). This provides a better average ρR measurement. Using eq. 3, the *dsr* values shown in the figure correspond to ρR values in the range 0.5-1.3 g/cm^2.

V. SUMMARY

A suite of neutron spectrometers, including an MRS and several nTOF detectors, have been implemented and extensively used on the NIF for measurements of the neutron spectrum in the energy range from 1.5 to about 20 MeV. The as-built performance of the spectrometers has been accurately calibrated *in situ* using a series of commissioning experiments in which DT and D^{3}He exploding pushers were utilized. The spectrometers, which perform well and meet the required accuracies for the Y_n, T_i, and *dsr* measurements, have been essential for diagnosing the implosion performance of DT layered implosions and for guiding NIC towards the first demonstration of ignition in the laboratory.

ACKNOWLEDGEMENTS

This work performed under the auspices of the U.S. Department of Energy by Lawrence Livermore National Laboratory under Contract DE-AC52-07NA27344. It was supported in part by LLE (414090-G) and FSC (415023-G).

[1]G.H Miller, E.I. Moses, and C.R. Wuest, Nucl. Fusion **44**, S228 (2004).

[2]V. Yu. Glebov *et al*., Rev. Sci. Inst. **77**, 10E715 (2006).
[3]D. Bleuel, these proceedings.
[4]F. Merrill, these proceedings.
[5]V. Yu. Glebov *et al.*, Rev. Sci. Inst. **81**, 10D325 (2010).
[6]C. Stoeckl, M. Cruz, V. Yu. Glebov, J.P. Knauer, R. Lauck, K. Marshall, C. Mileham, T.C. Sangster and W. Theobald, Rev. Sci. Inst. **81**, 10D302 (2010).
[7]Z.A. Ali *et al.*, Rev. Sci. Inst. **79**, 10E527 (2008).
[8]J.A. Frenje *et al.*, Rev. Sci. Inst. **72**, 854 (2001).
[9]J.A. Frenje *et al.*, Rev. Sci. Inst. **79**, 10E502 (2008).
[10]J.A. Frenje *et al.*, Phys. of Plasmas **17**, 056311 (2010).
[11]D.T. Casey, Diagnosing Inertial Confinement Implosions at OMEGA and the NIF Using Novel Neutron Spectrometry, PhD Thesis. MIT, February 2012
[12]D.C. Wilson, W.C. Mead, L. Disdier, M. houry, J.-L. Bourgade and T.J. Murphy, Nucl. Inst. Meth. A **488**, 400 (2002).
[13] E.I. Moses, J. Phys.: Conf. Ser. **112**, 012003 (2008).
[14]H. Brysk, Plasma Phys. **15**, 611 (1973).
[15]MCNPX Version 2.5.0 User's Manual (LA-CP-05-0369, April 2005) https://mcnpx.lanl.gov/
[16]M.J. Edwards *et al.*, Physics of Plasmas **18**, 051003 (2011).
[17]G.B. Zimmerman and W.L. Kruer, Comments Plasma Phys. Contr. Fusion **2** (1975) 85
[18]J.A. *Frenje et al*., Physics of Plasmas **16** (2009) 022702
[19]N.M. Hoffman, D.C. Wilson, H.W. Herrmann and C.S. Young, Rev. Sci. Inst. **81** (2010) 10D332
[20]S.P. Regan, private communication
[21]S.L. Nelson, D.A. Shaughnessy, L.A. Bernstein, D.L. Bleuel, C.J. Cerjan, K.J. Moody, D.H.G. Schneider and W. Stoeffl, IEEE Trans. Plasma Sci. **39** (2011) 1750-1753
[22]S. Le Pape et al., Bull. Am. Soc. 56, p 192 (2011)
[23]D.T. Casey *et al*., these proceedings.
[24]C. Forrest *et al.*, these proceedings.
[25]A.J. MacKinnon *et al.*, accepted for publication in PRL
[26]S.H. Glenzer et al., Plasma Phys. Cont. Fusion **54**, 045013 (2012).
[27]B. Spears *et al.*, Physics of Plasmas (2012) in press
[28]S.H. Glenzer *et al., Cryogenic thermonuclear fuel implosions on the National Ignition Facility*, submitted to PoP.